Available online at www.pelagiaresearchlibrary.com

Pelagia Research Library

Advances in Applied Science Research, 2015, 6(8):224-241

ISSN: 0976-8610
CODEN (USA): AASRFC

Second order slip flow of a MHD micropolar fluid over an unsteady stretching surface

K. Lakshmi Narayana and K. Gangadhar

Department of Mathematics, Acharya Nagarjuna University, Ongole, Andhra Pradesh, India

ABSTRACT

The unsteady, two dimensional, mixed convection flow of an viscous incompressible electrically conducting micropolar fluid over a vertical and impermeable stretching surface in the presence of MHD and second order slip flow when the buoyancy force assists or opposes the flow has been studied. Using the similarity transformations, the governing equations have been transformed into a system of ordinary differential equations. These differential equations are highly nonlinear which cannot be solved analytically. Therefore, bvp4c MATLAB solver has been used for solving it. Numerical results are obtained for the skin-friction coefficient, the couple wall stress and the local Nusselt number as well as the velocity, microrotation and temperature profiles for different values of the governing parameters, namely, material parameter, magnetic parameter, first order velocity slip parameter, second order velocity slip parameter and Eckert number.

Keywords: Unsteady Flow, Mixed Convection, Heat Transfer, Micropolar Fluid, MHD, Stretching Surface, Second order Slip Flow, Viscous Dissipation.

INTRODUCTION

Micropolar fluids are fluids of microstructure. They represent fluids consisting of rigid, randomly oriented, or spherical particles suspended in a viscous medium, where deformation of fluids particles is ignored. The dynamics of micropolar fluids, originated from the theory of Eringen [1-3], has been a popular area of research due to its application in a number of processes that occur in industry. Such applications include polymeric fluids, real fluids with suspensions, liquid crystal, animal blood, and exotic lubricants. Extensive reviews of theory of micropolar fluids and its applications can be found in review articles by Ariman et al. [4, 5] and recent books by Łukaszewicz [6] and Eringen [7].

According to most of the previous studies, the MHD flow has received the attention of many researchers due to its engineering applications. In metallurgy, for example, some processes involve the cooling of many continuous strips by drawing them through an electrically conducting fluid subject to a magnetic field (Kandasamy and Muhaimin [8]).This allows the rate of cooling to be controlled and final product with the desired characteristics to be obtained. Another important application of hydromagnetic flow in metallurgy is in the purification of molten metal’s from nonmetallic inclusions through the application of a magnetic field. Research has also been carried out by previous researchers on the flow and heat transfer effects of electrically conducting fluids such as liquid metals, water mixed with a little acid and other equivalent substance in the presence of a magnetic field. The studies have involved different geometries and different boundary conditions. Herdricha et al. [9] studied MHD flow control for plasma technology applications. They identified potential applications for magnetically controlled plasmas in the fields of space technology as well as in plasma technology. Seddeek et al. [10] investigated the similarity solution in MHD flow and heat transfer over a wedge taking into account variable viscosity and thermal conductivities. The magnetohydrodynamic (MHD) forced convection boundary layer flow of nanofluid over a horizontal stretching plate was investigated by Nourazar et al. [11] using homotopy perturbation method (HPM).

Unsteady free convection flows of dissipative fluids past an infinite plate have received a little attention because of non-linearity of the governing equations. Bhaskar Reddy and Bathaiah [12] studied the magnetohydrodynamic flow of a viscous incompressible fluid between a parallel flat wall and a long wavy wall. Neeraja and Bhaskar Reddy [13] investigated the MHD unsteady free convection flow past a vertical porous plate with viscous dissipation. Recently, El-Aziz [14] studied the mixed convection flow of a micropolar fluid from an unsteady stretching surface with viscous dissipation. Gangadhar [15] conclude that the local skin friction coefficient increases and local Nusselt number coefficient decreases in the presence of viscous dissipation. Aydin and Kaya [16] studied MHD mixed convection of a viscous dissipating fluid about a permeable vertical flat plate and found that the value of Richardson number determines the effect of the magnetic parameter on the momentum and heat transfer.

The non-adherence of the fluid to a solid boundary, also known as velocity slip, is a phenomenon that has been observed under certain circumstances (Yoshimura and Prudhomme [17]). It is a well-known fact that, a viscous fluid normally sticks to the boundary. But, there are many fluids, e.g. particulate fluids, rarefied gas etc., where there may be a slip between the fluid and the boundary (Shidlovskiy [18]). Beavers and Joseph [19] proposed a slip flow condition at the boundary. Andersson [20] considered the slip flow of a Newtonian fluid past a linearly stretching sheet. Ariel [21] investigated the laminar flow of an elastic-viscous fluid impinging normally upon a wall with partial slip of the fluid at the wall. Wang [22] undertook the study of the flow of a Newtonian fluid past a stretching sheet with partial slip and purportedly gave an exact solution. He reported that the partial slip between the fluid and the moving surface may occur in particulate fluid situations such as emulsions, suspensions, foams and polymer solutions. Fang et al [23] investigated the magnetohydrodynamic (MHD) flow under slip condition over a permeable stretching surface. Fang and Aziz [24] conclude that the combined effects of the two slips and mass transfer parameters greatly influence the fluid flow and shear stresses on the wall and in the fluid. Nandeppanavar et al. [25] analyze the second order slip flow and heat transfer over a stretching sheet. Sajid et al. [26] analyzed the stretching flow with general slip condition. Sahoo and Poncet [27] studied the Non-Newtonian boundary layer flow and heat transfer over an exponentially stretching sheet with partial slip boundary condition. Noghrehabadi *et al.* [28] analyzed the effect of partial slip on the flow and heat transfer of nanofluids past a stretching sheet. Zheng *et al.* [29] investigated the magnetohydrodynamic (MHD) flow and heat transfer over a stretching sheet with velocity slip and temperature jump. Sharma et al. [30] considered the velocity and temperature slip on the boundary. Sharma and Ishak [31] considered the Second order velocity slip flow model instead of no-slip at the boundary.

The present study investigates the unsteady mixed convection flow of a viscous incompressible electrically conducting micropolar fluid on a vertical and impermeable stretching sheet in the presence of MHD and second order slip flow. Using the similarity transformations, the governing equations have been transformed into a set of ordinary differential equations, which are nonlinear and cannot be solved analytically, therefore, bvp4c MATLAB solver has been used for solving it. The results for velocity, microrotation and temperature functions are carried out for the wide range of important parameters namely; material parameter, magnetic parameter, Eckert number and first order slip velocity parameter and second order velocity slip parameter. The skin friction, the couple wall stress and the rate of heat transfer have also been computed.

2. MATHEMATICAL FORMULATION

Consider an unsteady two dimensional, mixed convection boundary layer flow of a viscous incompressible micropolar fluid over an elastic, vertical and impermeable stretching sheet which emerges vertically in the upward direction from a narrow slot with velocity [32]

$$u_w(x,t) = \frac{ax}{1-\alpha_0 t} \tag{2.1}$$

where both a and α are positive constants with dimension per time. The positive x coordinate is measured along the stretching sheet with the slot as the origin and the positive y coordinate is measured normal to the sheet in the outward direction toward the fluid. The surface temperature T_w of the stretching sheet varies with the distance x from the slot and time t as

$$T_w(x,t) = T_\infty + \frac{bx}{(1-\alpha_0 t)^2} \tag{2.2}$$

where b is constant with dimension temperature over length and υ is the kinematic viscosity of the ambient fluid. It is apt to note here that, the expressions for $u_w(x,t)$ and $T_w(x,t)$ in Equations. (2.1) and (2.2) are valid only for time $t < \alpha_0^{-1}$ unless $\alpha_0 = 0$. Expression (2.1) for the velocity of the sheet $u_w(x,t)$ reflects that the elastic sheet which is fixed at the origin is stretched by applying a force in the positive x - direction and the effective stretching rate $\frac{a}{(1-\alpha t)}$ increases with time. With the same analogy the expression for the surface temperature $T_w(x,t)$ given by Equation (2.2) represents a situation in which the sheet temperature increases (reduces) if b is positive (negative) from T_∞ at the slot in proportion to x and such that the amount of temperature and concentration increase (reduction) along the sheet increases with time. A uniform magnetic field of strength B_0 is assumed to be applied in the positive y-direction normal to the plate. The magnetic Reynolds number of the flow is taken to be small enough so that the induced magnetic field is negligible. It is assumed that the radiation and Dufour effects are neglected in the energy equation. It is further assumed that the fluid properties are taken to be constant except for the density variation with the temperature in the buoyancy terms. Under the usual boundary layer approximation, the governing equations are

Continuity equation

$$\frac{\partial u}{\partial x}+\frac{\partial v}{\partial y}=0 \tag{2.3}$$

Linear momentum equation

$$\frac{\partial u}{\partial t}+u\frac{\partial u}{\partial x}+v\frac{\partial u}{\partial y}=\left(\frac{\mu+\kappa}{\rho}\right)\frac{\partial^2 u}{\partial y^2}-\frac{\sigma B_0^2}{\rho}u+\frac{\kappa}{\rho}\frac{\partial N}{\partial y}+g\beta_T\left(T-T_\infty\right) \tag{2.4}$$

Angular momentum equation

$$\rho j\left(\frac{\partial N}{\partial t}+u\frac{\partial N}{\partial x}+v\frac{\partial N}{\partial y}\right)=\gamma^*\frac{\partial^2 N}{\partial y^2}-\kappa\left(2N+\frac{\partial u}{\partial y}\right) \tag{2.5}$$

Energy equation

$$\frac{\partial T}{\partial t}+u\frac{\partial T}{\partial x}+v\frac{\partial T}{\partial y}=\alpha_1\frac{\partial^2 T}{\partial y^2}+\left(\frac{\mu+\kappa}{\rho c_p}\right)\left(\frac{\partial u}{\partial y}\right)^2 \tag{2.6}$$

The boundary conditions for the velocity, Angular Velocity and temperature fields are

$$u=u_w+U_{Slip}, v=0, N=0, T=T_w \quad \text{at} \quad y=0$$
$$u\to 0, N\to 0, T\to T_\infty \quad \text{as} \quad y\to\infty \tag{2.7}$$

Where U_{slip} is the slip velocity at the wall. The Wu's Slip velocity model (Valid for arbitrary Kundsen number's) is used and is given as follows

$$U_{Slip}=\frac{2}{3}\left[\frac{3-\alpha l^2}{\alpha}-\frac{3}{2}\frac{1-l^2}{K_n}\right]\lambda_1\frac{\partial u}{\partial y}-\frac{1}{4}\left[l^4+\frac{2}{K_n^2}(1-l^2)\right]\lambda_1^2\frac{\partial^2 u}{\partial y^2}$$
$$=A\frac{\partial u}{\partial y}+B\frac{\partial^2 u}{\partial y^2} \tag{2.8}$$

Where u and v are the velocity components in the x - and y - directions, respectively, T is the fluid temperature in the boundary layer, N is the component of the microrotation vector normal to the x-y plane, σ is the spin-gradient viscosity and $\alpha_1(=k/\rho c_p)$ is the thermal diffusivity with k is the fluid thermal conductivity, c_p is the heat capacity pressure, respectively.
The continuity equation (2.3) is satisfied by the Cauchy Riemann equations

$$u = \frac{\partial \psi}{\partial y} \text{ and } v = -\frac{\partial \psi}{\partial x} \tag{2.9}$$

where $\psi(x, y)$ is the stream function.
In order to transform equations (2.4), (2.5) (2.6) and (2.7) into a set of ordinary differential equations, the following similarity transformations and dimensionless variables are introduced.

$$\eta = \sqrt{\frac{a}{\upsilon(1-\alpha_0 t)}}y, \psi = \sqrt{\frac{\upsilon a}{1-\alpha_0 t}}xf(\eta), N = \sqrt{\frac{a^3}{\upsilon(1-\alpha_0 t)^3}}xh(\eta)$$
$$T = T_\infty + \frac{bx}{(1-\alpha_0 t)^2}\theta(\eta), A = \frac{\alpha_0}{a}, K = \frac{\kappa}{\mu}$$
$$M = \frac{\sigma B_0^2}{\rho \alpha_0}, \Pr = \frac{\upsilon}{\alpha_1}, Gr_x = \frac{g\beta_T(T_w - T_\infty)x^3}{\upsilon^2}, \mathrm{Re}_x = \frac{u_w x}{\upsilon} \tag{2.10}$$
$$\lambda_0 = \frac{\gamma^*}{\mu j}, \zeta = \frac{g\beta_T b}{a^2} = \frac{Gr_x}{\mathrm{Re}_x^2}$$
$$B = \frac{\upsilon(1-\alpha_0 t)}{jb} = \frac{\upsilon x}{jU_w}, Ec = \frac{U_w^2}{c_p(T_w - T_\infty)}$$

where $f(\eta)$ is the dimensionless stream function, θ is the dimensionless temperature, η is the similarity variable, A is the unsteadiness parameter, M is the magnetic parameter, Ec is the Eckert number, Gr_x is the thermal Grashof number, ζ is the thermal buoyancy parameter, λ_0 and B are the dimensionless parameters, Re_x is the local Reynolds number, Pr is the Prandtl number.

In view of equations (2.9) and (2.10), the equations (2.4), (2.5) and (2.6) transform into

$$(1+K)f''' + ff'' - (f')^2 + Kh' - Mf' - \frac{A}{2}(2f' + \eta f'') + \zeta\theta = 0 \tag{2.11}$$

$$\lambda_0 h'' + fh' - f'h - KB(2h + f'') - \frac{A}{2}(3h + \eta h') = 0 \tag{2.12}$$

$$\frac{1}{\Pr}\theta'' + f\theta' - f'\theta - \frac{A}{2}(4\theta + \eta\theta') + Ec(1+K)(f'')^2 = 0 \tag{2.13}$$

The corresponding boundary conditions are

$$f(0) = 0, f'(0) = 1 + \gamma f''(0) + \delta f'''(0), h(0) = 0, \theta(0) = 1$$
$$f' = h = \theta = 0 \quad \text{as} \quad \eta \to \infty \tag{2.15}$$

where the primes denote differentiation with respect to η and the $\gamma = A\sqrt{\frac{a}{\upsilon(1-\alpha_0 t)}}(>0)$ is the first order velocity slip parameter, $\delta = B\left(\frac{a}{\upsilon(1-\alpha_0 t)}\right)(<0)$ is the second order velocity slip parameter

The physical quantities of interest are the skin friction coefficient C_{fx}, the local couple wall stress M_{wx} and the local Nusselt number Nu_x which are defined as

$$C_{fx} = \frac{2}{\rho U_w^2}\left[(\mu+\kappa)\left(\frac{\partial u}{\partial y}\right)_{y=0} + \kappa (N)_{y=0} \right] = 2(1+K)\mathrm{Re}_x^{-1/2} f''(0) \quad (2.16)$$

$$M_{wx} = \gamma \left(\frac{\partial N}{\partial y}\right)_{y=0} = \frac{\gamma a U_w}{\upsilon(1-\alpha t)} h'(0) \quad (2.17)$$

$$Nu_x = -\frac{x}{T_w - T_\infty}\left(\frac{\partial T}{\partial y}\right)_{y=0} = -\mathrm{Re}_x^2 \theta'(0) \quad (2.18)$$

Our main aim is to investigate how the values of $f''(0)$, $h'(0)$ and $-\theta'(0)$ vary in terms of the various parameters.

3 SOLUTION OF THE PROBLEM

The set of equations (2.11) to (2.13) were reduced to a system of first-order differential equations and solved using a MATLAB boundary value problem solver called **bvp4c**. This program solves boundary value problems for ordinary differential equations of the form $y' = f(x, y, p), a \le x \le b$, by implementing a collocation method subject to general nonlinear, two-point boundary conditions $g(y(a), y(b), p)$. Here ***p*** is a vector of unknown parameters. Boundary value problems (BVPs) arise in most diverse forms. Just about any BVP can be formulated for solution with **bvp4c**. The first step is to write the *ODEs* as a system of first order ordinary differential equations. The details of the solution method are presented in Shampine and Kierzenka[33].

RESULTS AND DISCUSSION

The governing equations (2.11) - (2.13) subject to the boundary conditions (2.14) are integrated as described in section 3. In order to get a clear insight of the physical problem, the velocity, angular velocity, temperature and concentration have been discussed by assigning numerical values to the parameters encountered in the problem.

Table.1 Comparison for the values of $-\theta'(0)$ for Δ=Ec=γ=δ=0 and various values of A, ζ and Pr with Ishak et al.[34]

A	ζ	Pr	$-\theta'(0)$ Ishak et al.[34]	$-\theta'(0)$ Present results
0	0	0.72	0.8086	0.8087
0	0	1	1.0000	1.0000
0	0	3	1.9237	1.9237
0	0	10	3.7207	3.7207
0	0	100	12.294	12.2941
0	1	1	1.0873	1.0873
0	2	1	1.1423	1.1423
0	3	1	1.1853	1.1853
1	0	1	1.6820	1.6820
1	1	1	1.7039	1.7039
1	-0.5	10	5.5585	5.5585
1	0.5	10	5.5690	5.5690

Physically $\zeta > 0$ means heating of the fluid or cooling of the surface (assisting flow), $\zeta < 0$ means cooling of the fluid or heating of the surface (opposing flow) and $\zeta = 0$ means the absence of free convection currents (forced convection flow). Figs. 1-3 illustrate the axial velocity, angular velocity and temperature fields for different values of the magnetic parameter (*M*). It is observed that for both positive (assisting flow) and negative (opposing flow) ζ that the axial velocity $f'(\eta)$ and angular velocity $h(\eta)$ decrease while the temperature $\theta(\eta)$ increases with an increase in the magnetic parameter. The magnetic parameter is found to retard the velocity at all points of the flow field. It is because that the application of transverse magnetic field will result in a resistive type force (Lorentz force) similar to drag force which tends to resist the fluid flow and thus reducing its velocity.

The axial velocity, angular velocity and temperature profiles in the case of assisting and opposing flows and various values of the first order velocity slip parameter γ and the second order velocity slip parameter δ are presented in Figs. 4-9. It is found that for both positive (assisting flow) and negative (opposing flow) ζ, the present findings are similar to results reported by Sharma and Ishak [31] that is axial velocity $f'(\eta)$ decrease while the temperature $\theta(\eta)$ increases with an increase in the γ and Further angular velocity $h(\eta)$ decreases with γ and δ.

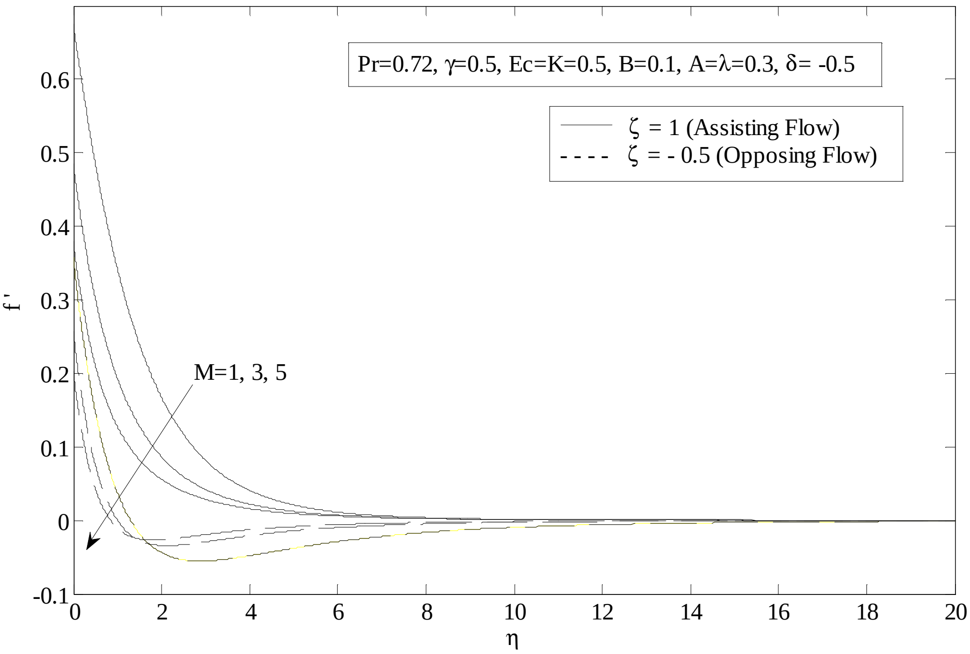

Fig.1 Velocity for different values of *M*

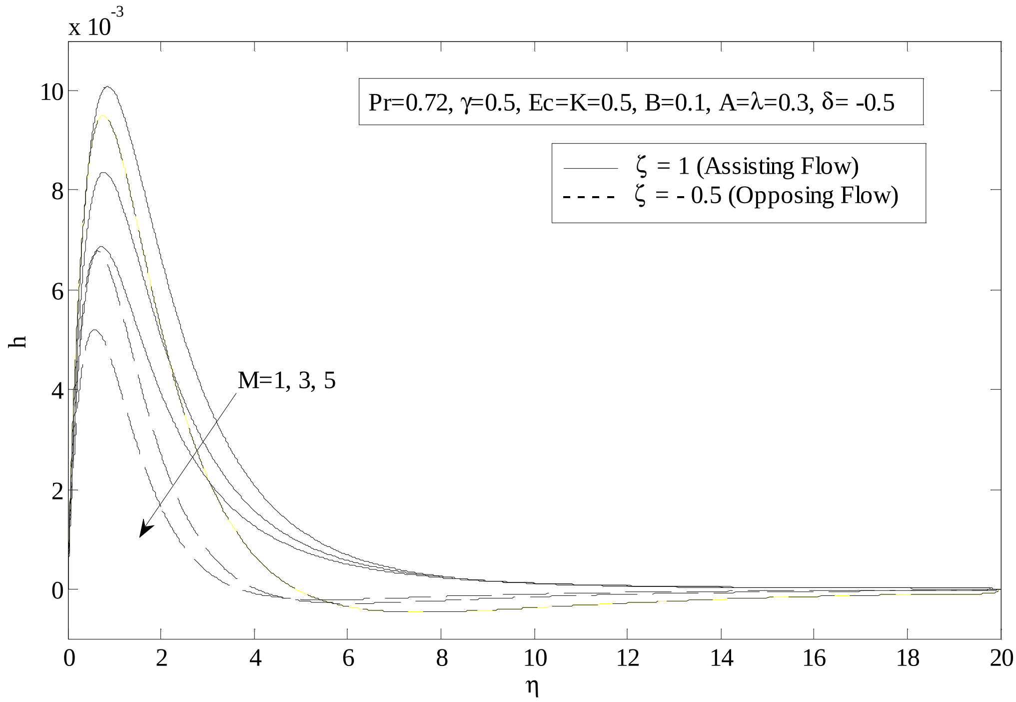

Fig.2 Angular velocity for different values of *M*

Representative axial velocity, angular velocity, temperature and concentration profiles in the case of assisting and opposing flows and various values of the micropolar parameter *K* are presented in Figs. 10-12. It is found that for both positive (assisting flow) and negative (opposing flow) ζ that the raising the values of K the present results similar to those results of El-Aziz [14] that is the axial velocity $f'(\eta)$ and angular velocity $h(\eta)$ increase while the temperature $\theta(\eta)$ decreases with an increase in the micropolar parameter K, but the effect of K on the velocity, temperature fields is more pronounced in the case of opposing flow. When $K=0$ (Newtonian fluid) there is no angular velocity, and as K increases, the angular velocity is greatly induced. Further, the micropolar parameter K demonstrates a more pronounced influence on the axial and angular velocities $f'(\eta)$ and $h(\eta)$ respectively, than that on the temperature $\theta(\eta)$. Moreover, it is seen from Figs. 10 and 11 that the smaller the K, the thinner the momentum and angular momentum boundary layer thickness while the opposite trend is true for the thermal boundary layer as obvious from Fig. 12.

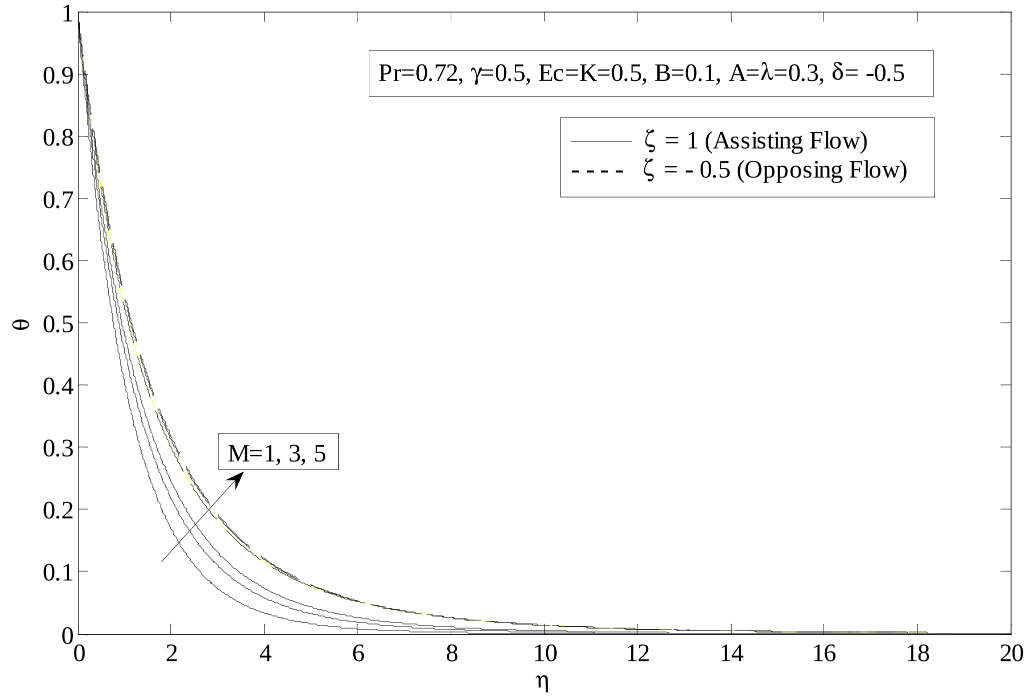

Fig.3 Temperature for different values of *M*

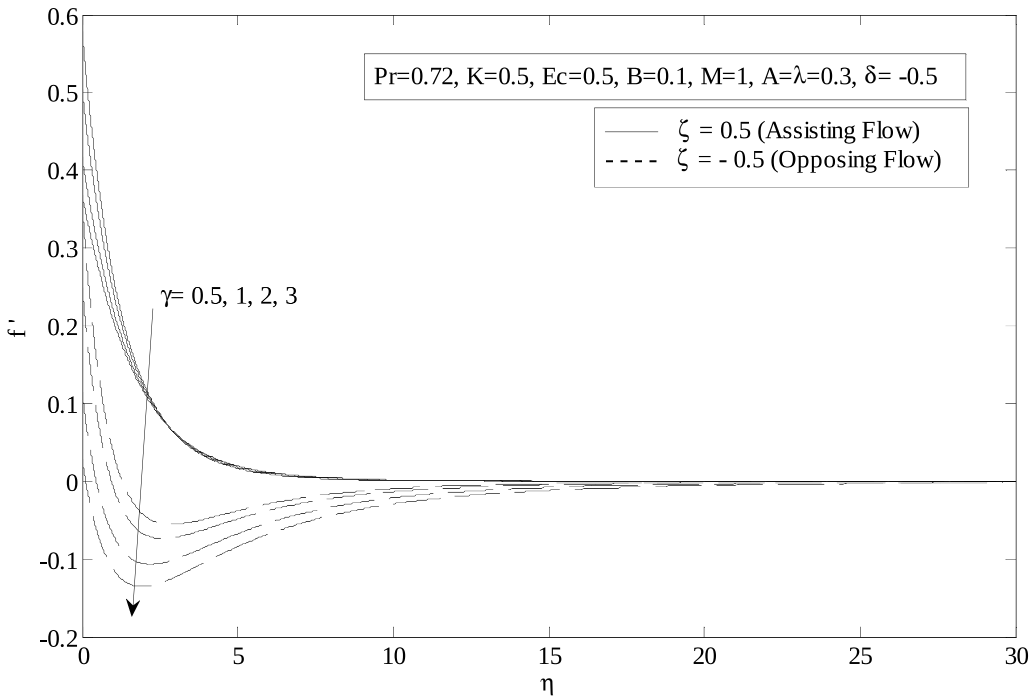

Fig.4 Velocity for different values of *γ*

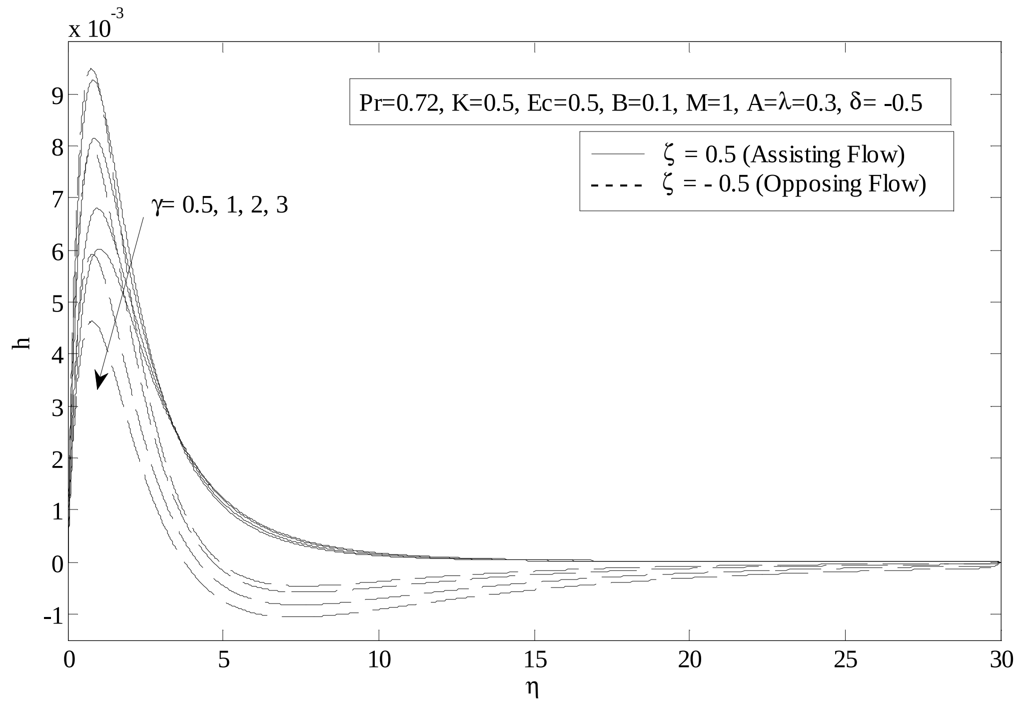

Fig.5 Angular velocity for different values of γ

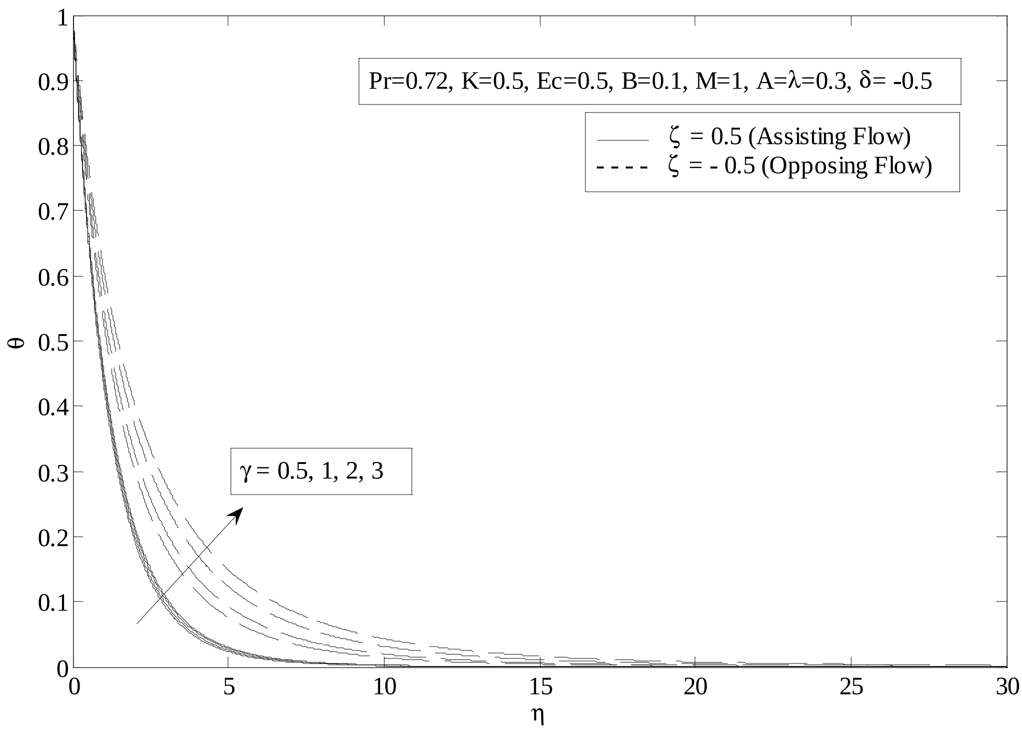

Fig.6 Temperature for different values of γ

Figs. 13-15 are the plot of the velocity, angular velocity and temperature distribution with η for various values of Eckert number *Ec* in the case of assisting and opposing flows. It is known that the viscous dissipation produces heat due to drag between the fluid particles and this extra heat causes an increase of the initial fluid temperature (see Fig.15). This increase of temperature causes an increase of the buoyant force. Also, there is a continuous interaction between the viscous heating and the buoyant force. This mechanism produces different results in the assisting (upward) and opposing (downward) flow. In the assisting (opposing) flow, the increase in the values of positive (negative) Ec will increase the buoyant force in the upward (downward) direction which results in an increase in the fluid velocity as shown in Fig. 13. The positive (Ec > 0) and negative (Ec < 0) Eckert numbers assists the upward ($\zeta > 0$ and hence Ec >0) and downward ($\zeta < 0$ and hence Ec < 0) flow, respectively as shown in Fig. 13.

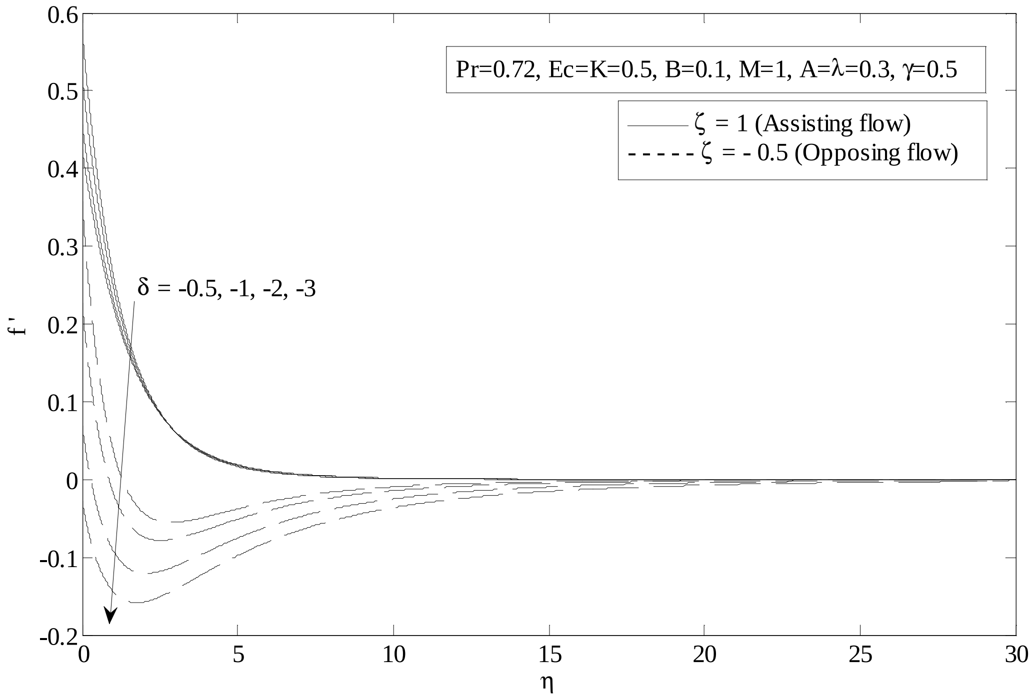

Fig.7 Velocity for different values of δ

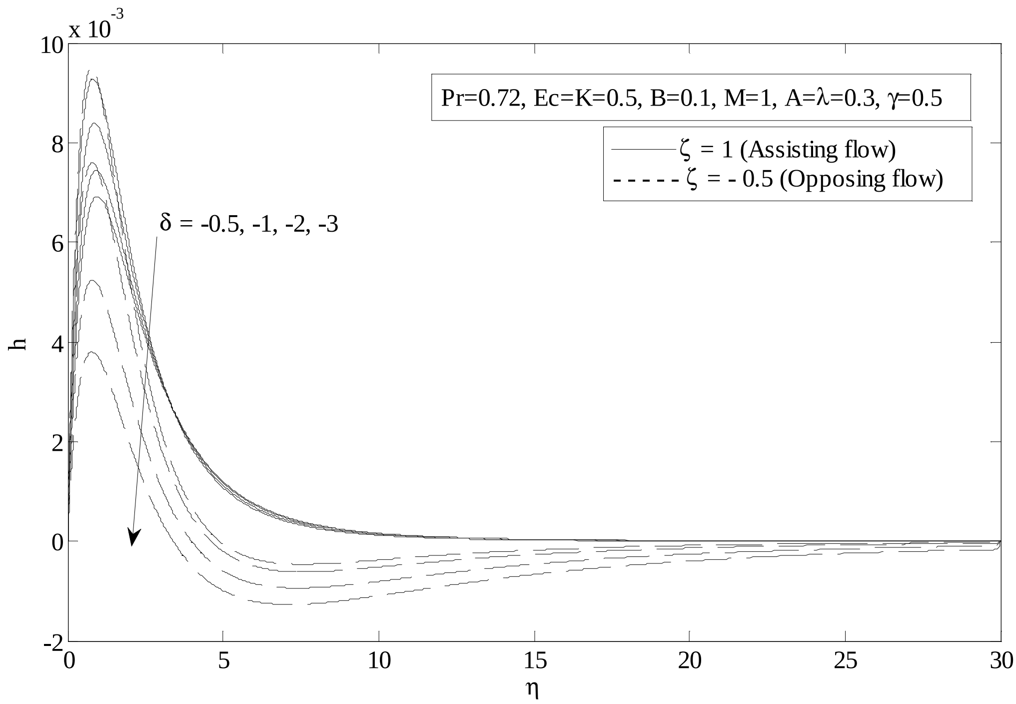

Fig.8 Angular velocity for different values of δ

It is noted from Fig. 14 that the angular velocity $h(\eta)$ first decreases with an increase in the Eckert number. According to the definition of Eckert number, a positive Ec corresponds to fluid heating (heat is being supplied across the walls into the fluid) case ($T_w > T_\infty$) so that the fluid is being heated whereas a negative Ec means that the fluid is being cooled. From Fig. 15 it is seen that the dimensionless temperature increases when the fluid is being heated (Ec >0) but decrease when the fluid is being cooled (Ec < 0). For Ec < 0 the dimensionless fluid temperature $T_w < T_\infty$ decreases monotonically with η, from unity at the wall towards its free-stream value.

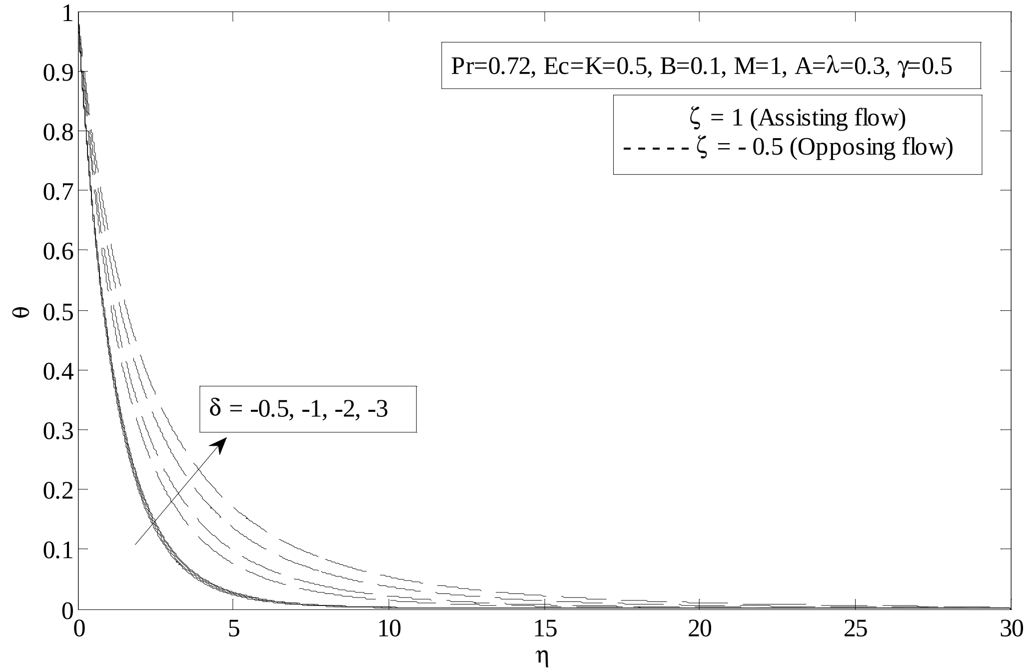

Fig.9 Temperature for different values of *δ*

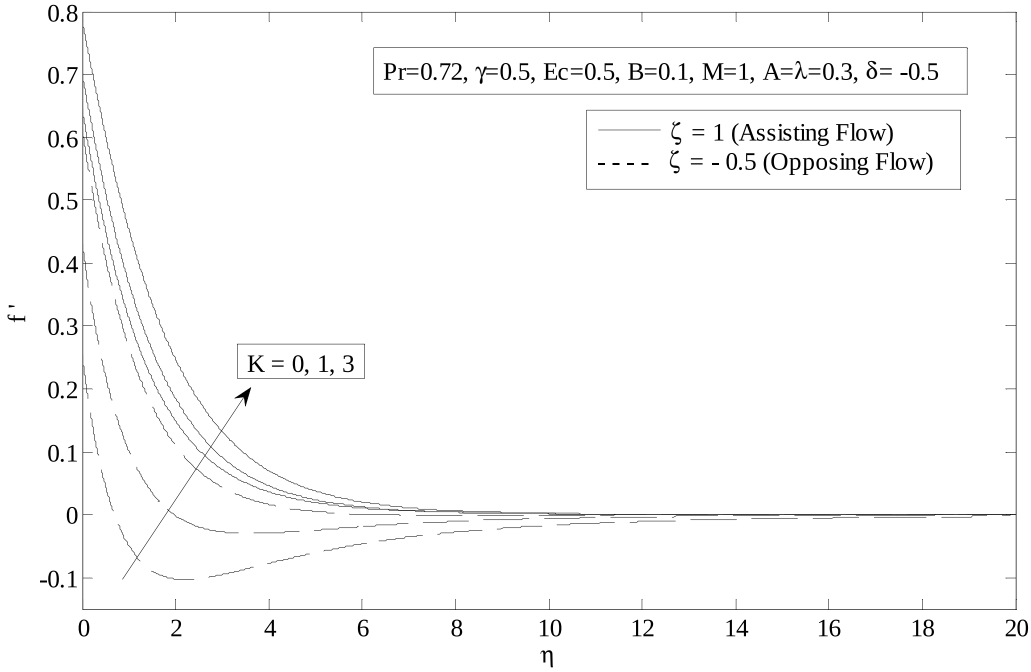

Fig.10 Velocity for different values of *K*

It is noted from the definition of θ that this behavior implies the monotonous decrease in the actual fluid temperature in the horizontal direction from the sheet temperature T_w to the free-stream temperature. On the other hand, for Ec < 0 (i.e. $T_w < T_\infty$) the dimensionless fluid temperature θ decreases with η rapidly at first, arriving at a negative minimum value, for Ec = -4 and then increases more gradually to its free surface value. Correspondingly, the actual fluid temperature in the horizontal direction increases at first from the surface temperature T_w to a maximum value and then decrease to its free-stream value. It should be noted that for the fluid cooling case (Ec < 0) a negative θ indicates the excess of actual fluid temperature T over that at the plate because of the viscous dissipation effect.

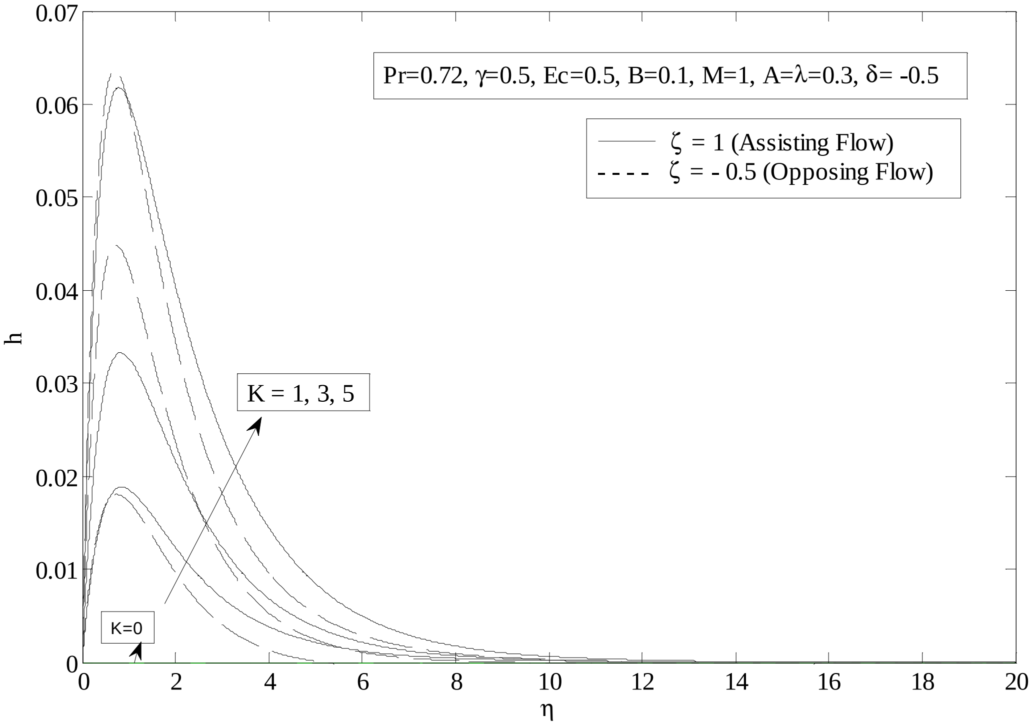

Fig.11 Angular velocity for different values of *K*

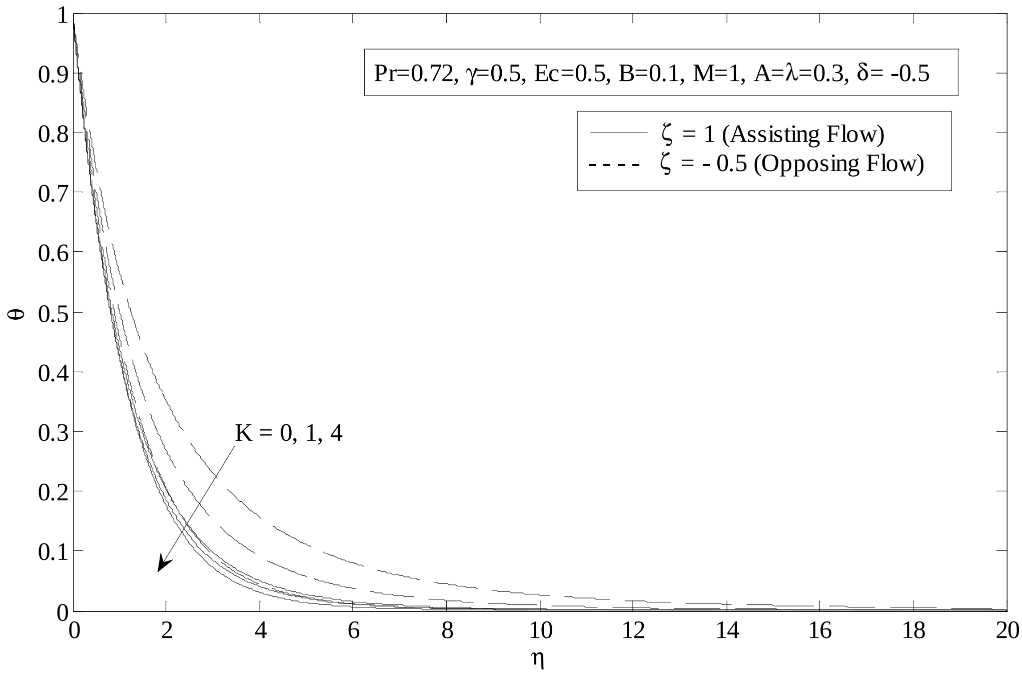

Fig.12 Temperature for different values of *K*

Fig. 16-18 shows the variation of the skin friction, couple wall stress and Nusselt number with for different values of magnetic parameter and Eckert number. It is observed that the skin friction increases with an increase in the Ec for both assisting and opposing flow cases these finding are similar to the results reported by El-Aziz [14]. In addition, the effect of viscous dissipation on skin friction is more pronounced for lower values of *M*, It is also observed that the local skin friction coefficient of buoyancy assisting flow is higher than that of buoyancy opposing flow for all values of *M* and Ec and couple wall stress decreases with increasing the Ec these findings are similar to the results reported by El-Aziz [14], Further, viscous dissipation demonstrates a more pronounced influence on the wall couple stress in the opposing flow than that of assisting flow (See Fig. 17).

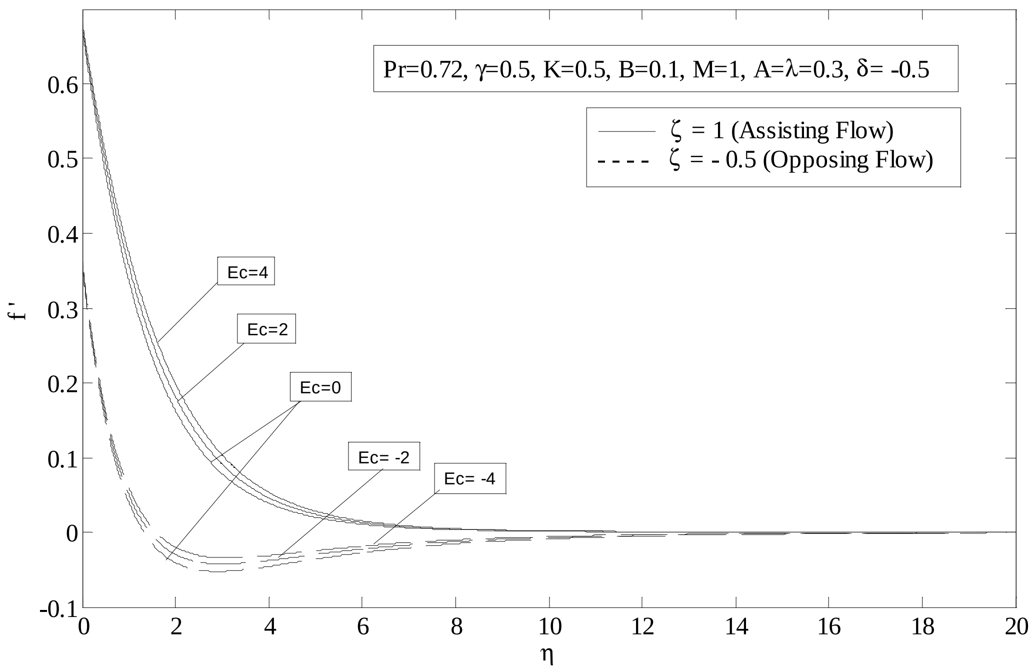

Fig.13 Velocity for different values of *Ec*

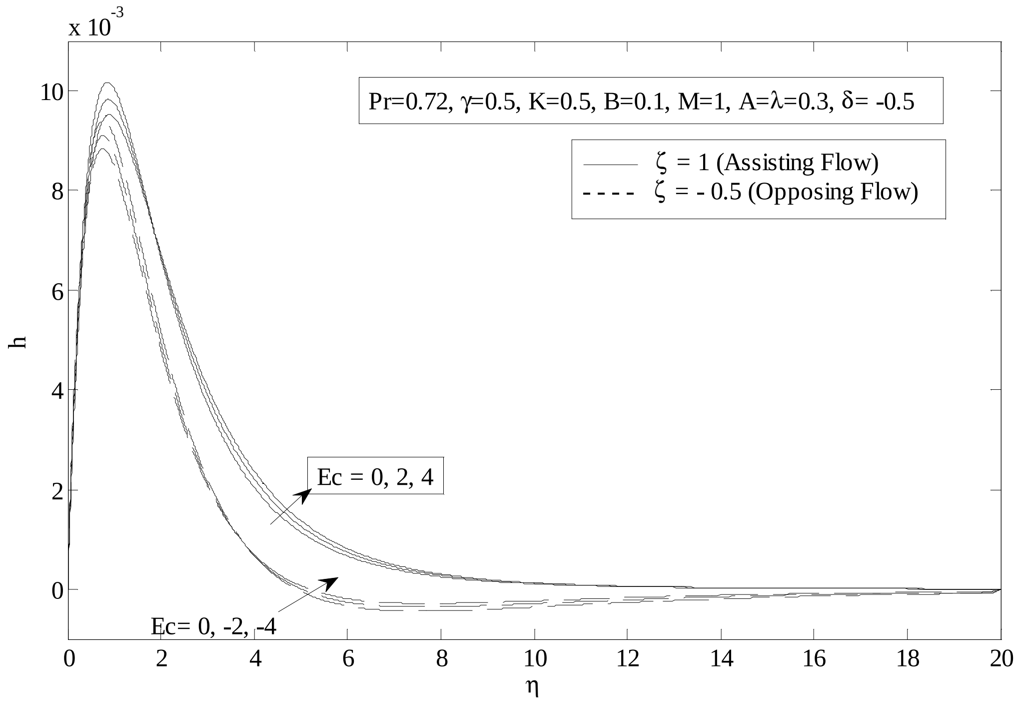

Fig.14 Angular velocity for different values of *Ec*

It is observed that the heat transfer rate decreases with an increase in the Eckert number, Further, viscous dissipation demonstrates a more pronounced influence on the Nusselt number in the opposing flow than that of assisting flow and also, increases with increasing the Magnetic parameter in the case of assisting flow and decreases in the case of opposing flow (See Fig.18). Fig. 19(a)-19(b) depicts the variation of the skin friction for different values of γ and δ. It is noticed that the skin friction increases with an increasing in δ in the range of $0.5 \leq \gamma \cong 1.7$ and decreases with increasing δ in the range of $1.7 \cong \gamma \leq 3$ in the case of assisting flow. It is observed that the skin friction increases with an increase in the parameters γ or δ in the case of opposing flow.

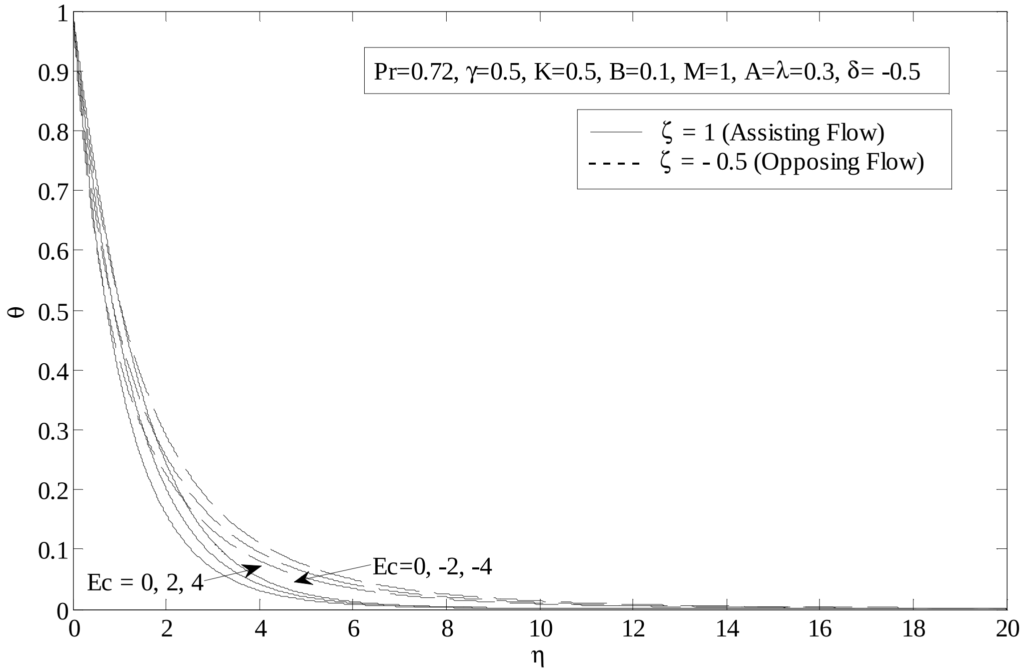

Fig.15 Temperature for different values of *Ec*

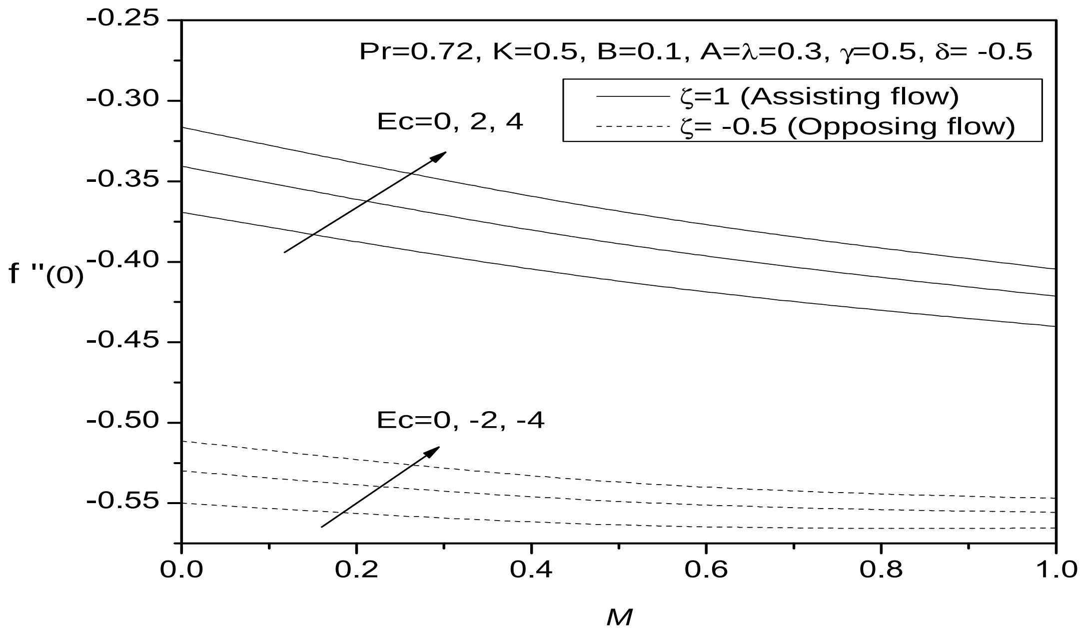

Fig.16 Skin friction for different values of *M* and *Ec*

Variations of the wall couple stress and Nusselt number for the different values of γ and δ are presented in Figs. 20(a)-21(b). It is noticed that the skin friction and Nusselt number decreases with an increasing in δ in the range of $0.5 \leq \gamma \cong 1.7$ and increases with increasing δ in the range of $1.7 \cong \gamma \leq 3$ in the case of assisting flow. It is observed that the skin friction and Nusselt number decreases with an increase in the parameters γ or δ in the case of opposing flow. Table.1 shows that the present results perfect agreement to the previously published data (Ref.34).

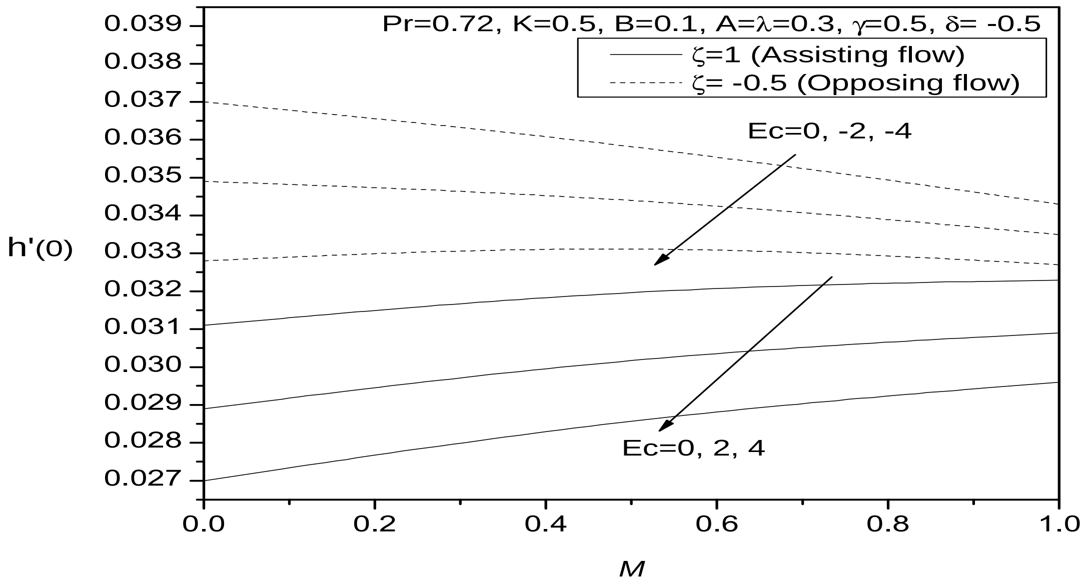

Fig.17 couple wall stress for different values of *M* and *Ec*

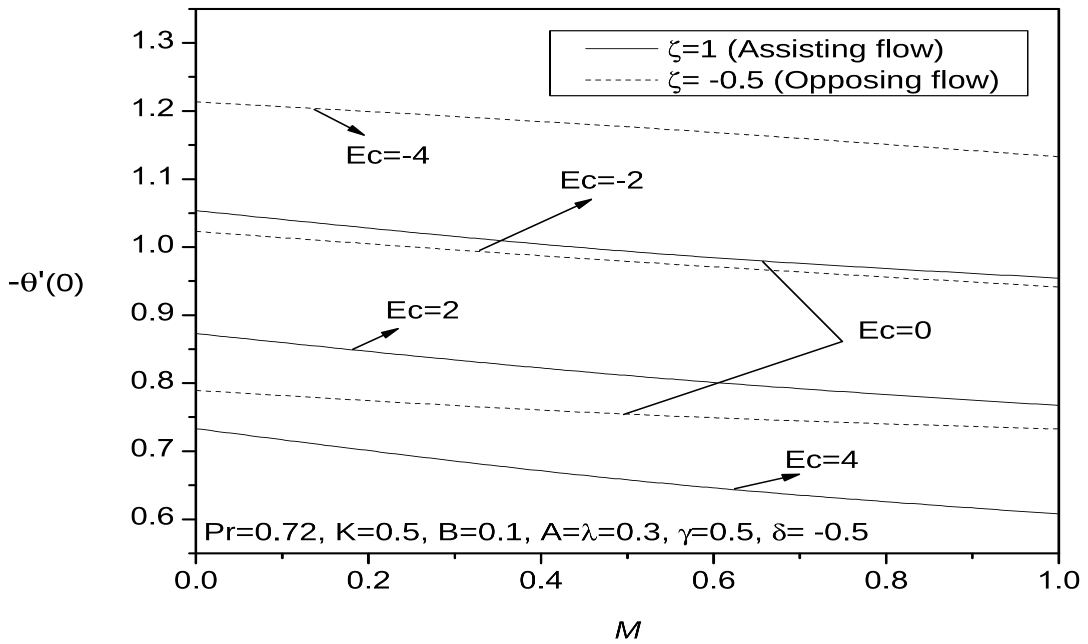

Fig.18 Nusselt number for different values of *M* and *Ec*

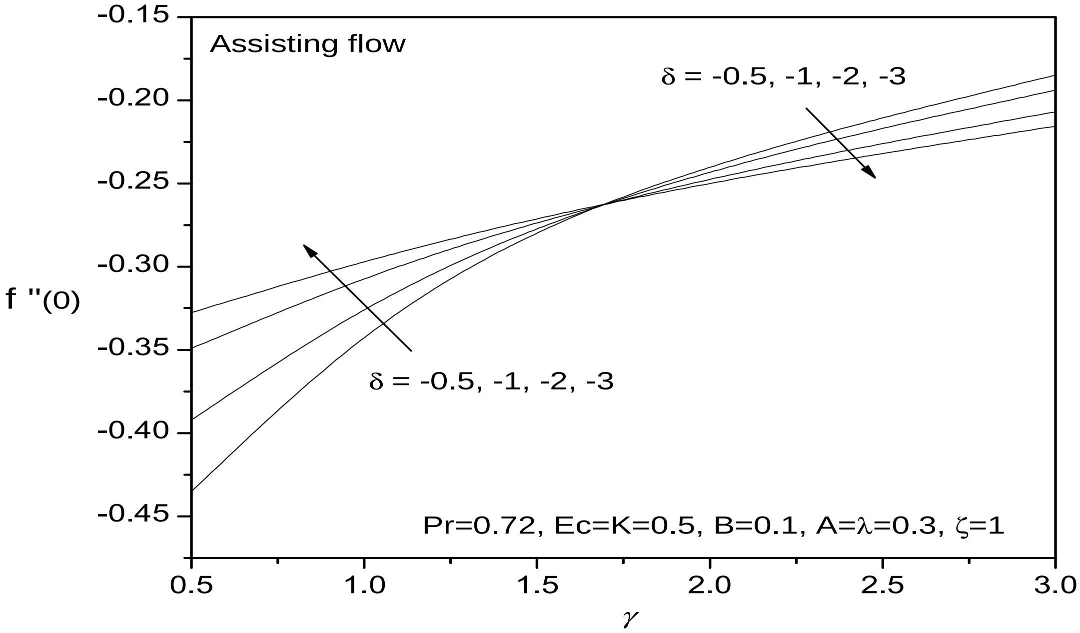

Fig.19 (a) Skin friction for different values of γ and δ for assisting flow

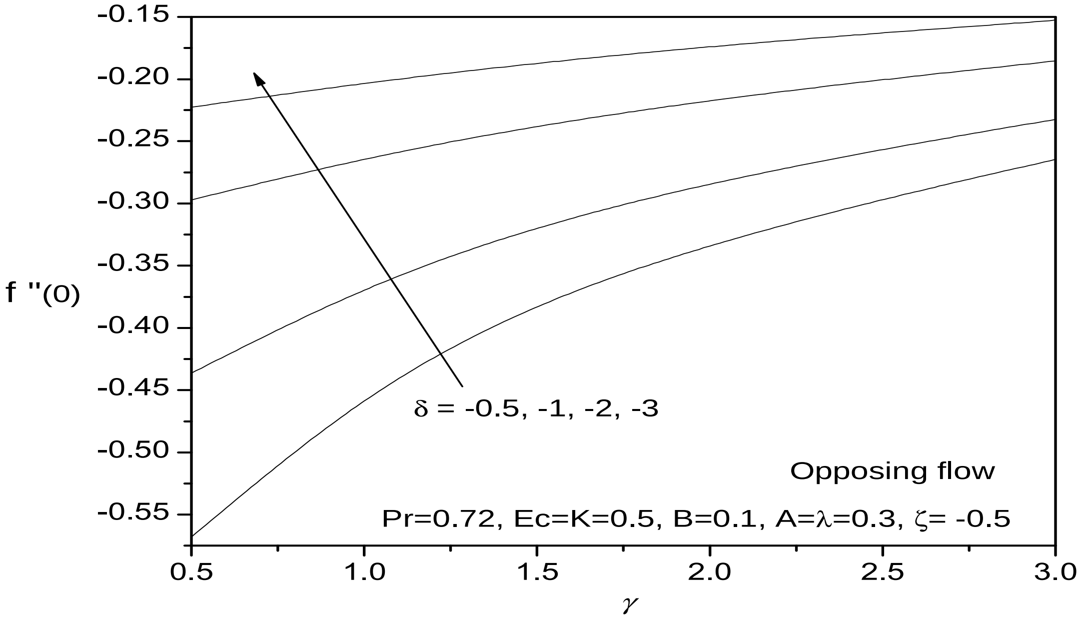

Fig.19 (b) Skin friction for different values of γ and δ for opposing flow

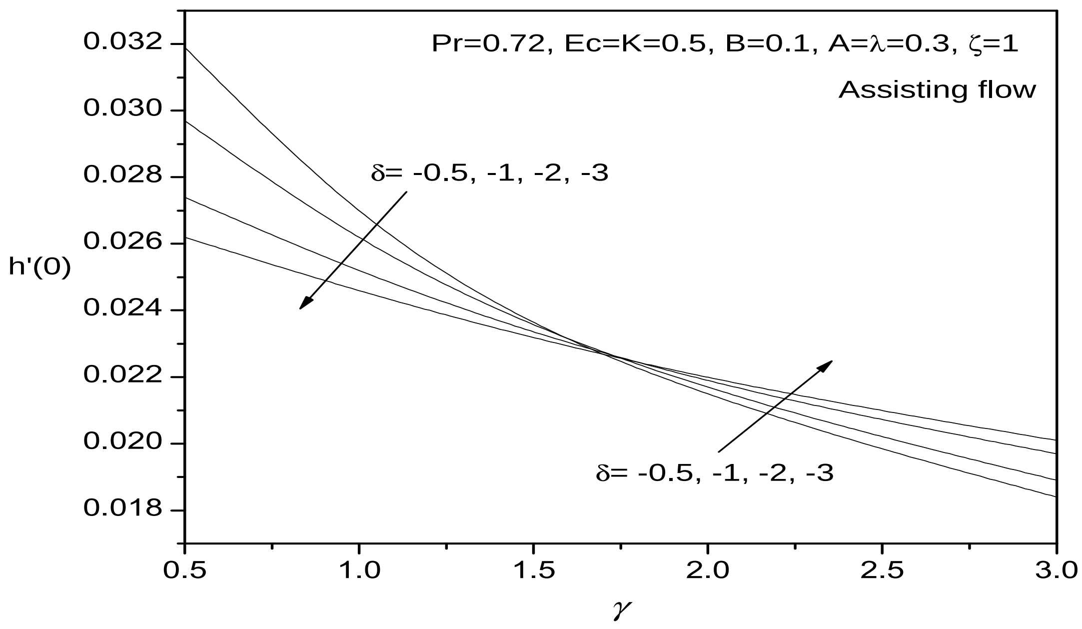

Fig.20(a) couple wall stress for different values of γ and δ for assisting flow

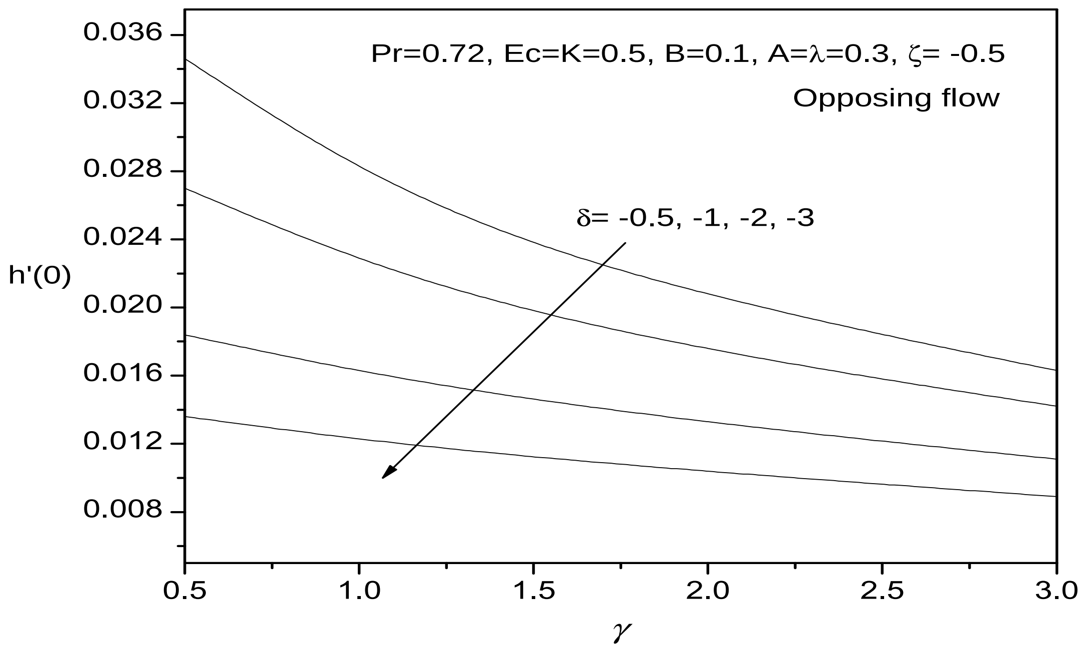

Fig.20(b) couple wall stress for different values of γ and δ for opposing flow

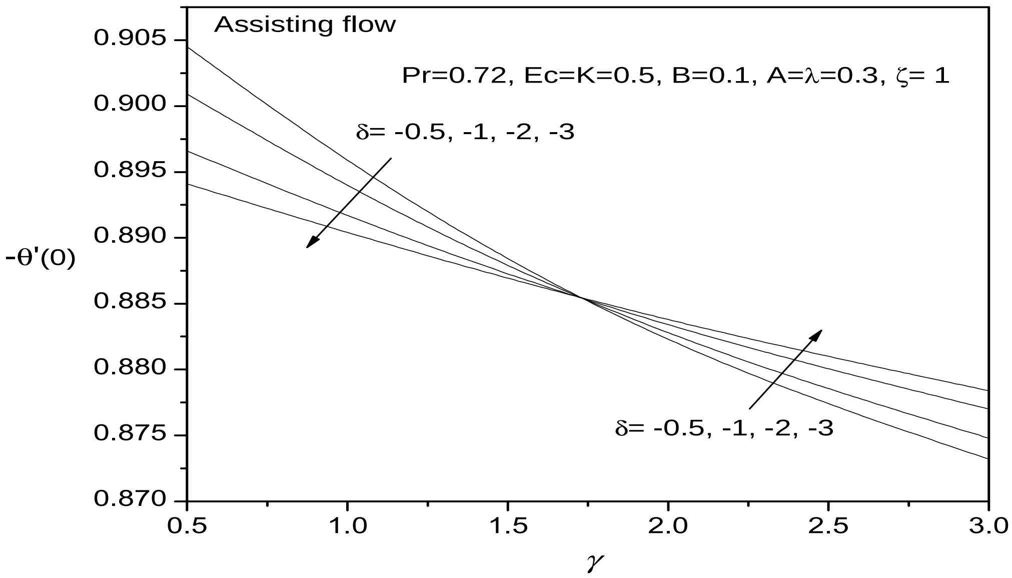

Fig.21(a) Nusselt number for different values of γ and δ for assisting flow

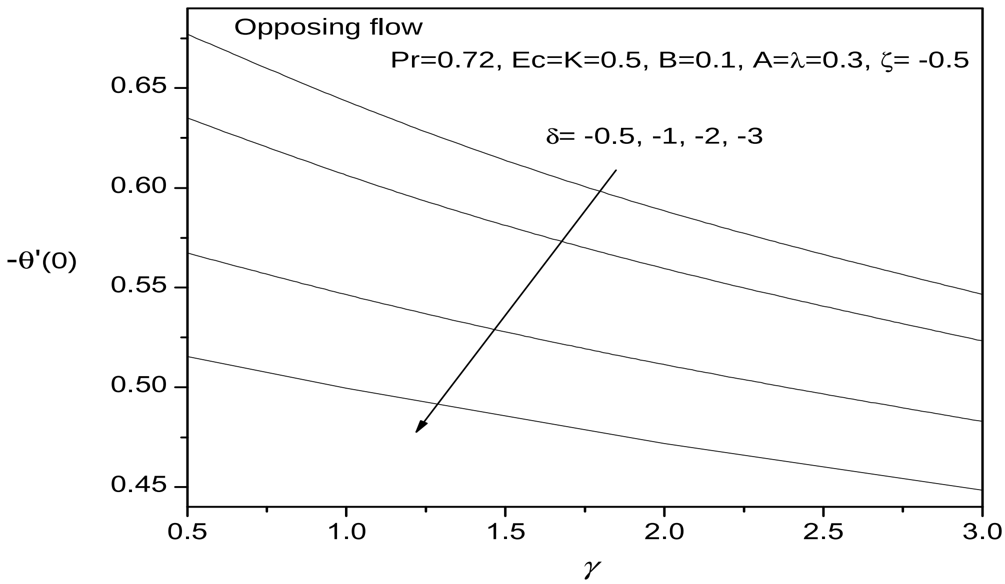

Fig.21(b) Nusselt number for different values of γ and δ for opposing flow

CONCLUSION

In the present prater, the unsteady mixed convection flow of a viscous incompressible electrically conducting micropolar fluid on a vertical and impermeable stretching surface by taking MHD and second order slip flow into account, are analyzed. The governing equations are approximated to a system of non-linear ordinary differential equations by similarity transformation. Numerical calculations are carried out for various values of the dimensionless parameters of the problem. It has been found that

1. The velocity and angular velocity decreases as well as temperature increases with an increase in the magnetic parameter in both assisting and opposing flows.
2. The first order slip parameter and second order slip parameter reduces the velocity and angular velocity, and enhances the temperature in both assisting and opposing flows.
3. The skin friction enhances the first order slip parameter or second order slip parameter and decreases the first order slip parameter and second order slip parameter for opposing flows.

REFERENCES

[1] Eringe, A. C., (**1964**), *International Journal of Engineering Science*, Vol. 2, pp. 205-217.
[2] Eringen, A. C., (**1966**), Vol. 16, pp. 1-18.
[3] Eringen, A. C., (**1972**), *Journal of Mathematical Analysis and Applications*, Vol. 38, No. 2, pp. 480-496.
[4] Ariman, T., Turk, M. A., and Sylvester, N. D., (**1973**), *International Journal of Engineering Science*, Vol. 11, No. 8, pp. 905-930.
[5] Ariman, T., Turk, M. A., and Sylvester, N. D., (**1974**), *International Journal of Engineering Science*, Vol. 12, No. 4, pp. 273-293.
[6] Łukaszewicz, G., (**1999**), Birkh¨auser, Boston, Mass, USA, Theory and applications.
[7] Eringen, A. C., (**2001**), II. Fluent Media, Springer, NewYork, NY, USA.
[8] Kandasamy, R., and Muhaimin, I., (**2010**), *Transport in Porous Media*, Vol. 84, No. 2, pp. 549–568.
[9] Herdricha, G., Auweter-Kurtza, M., Fertiga, M., Nawaza, A., and Petkowa, D., (**2006**), *Vacuum*, Vol. 80, pp. 1167–1173.
[10] Seddeek, M. A., Afify, A. A., and Hanaya, M. A., (**2009**), *Applications and Applied Mathematics*, Vol. 4, pp. 301–313.
[11] Nourazar, S.S., Matin, M.H., and Simiari, M., (**2011**), *J. Appl. Math.*, 2011: doi:10.1155/2011/876437.
[12] Bhaskar Reddy, N. and Bathaiah, D., *Defence Sci., Journal*, 31, No.4, 315-322, **1981**.
[13] Neeraja, A. and Bhaskar Reddy, N., (**2008**), *Ultra Science*, Vol.20, No.1(M), pp.183-194.
[14] Mohamed Abd El-Aziz, (**2013**), *Journal of the Egyptian Mathematical Society*, Vol. 21, pp.385–394.
[15] Gangadhar, K., (**2012**), *Int. J. of Appl. Math and Mech., Vol.* 8 (18), pp. 90-100.
[16] Aydin, O., and Kaya, A., (**2009**), *Applied Mathematical Modelling*, Vol. 33, No. 11, pp. 4086–4096.
[17] Yoshimura, A. and Prudhomme, R.K., (**1998**), *J. Rheol.*, Vol.32, pp.53-67.
[18] Shidlovskiy, V.P., (**1967**), New York: American Elsevier Publishing Company Inc.
[19] Beavers, G.S. and Joseph, D.D., (**1967**), *J. Fluid Mech.*, Vol.30, pp.197–207.
[20] Andersson, H.I., (**2002**), *Acta. Mech.*, Vol.158, pp.121-125.
[21] Ariel, P.D., (**2008**), *J. Appl. Math. Mech. (ZAMM)*, Vol.88, pp.320–324.
[22] Wang, C.Y., (**2002**), *Chem. Eng. Sci., Vol.*57, pp.3745-3747.
[23] Fang, T., Zhang, J. and Yao, S., (**2009a**), *Commun. Nonlinear Sci. Numer. Simulat.*, Vol.17, pp.3731-3737.
[24] Fang, T., and Aziz, A. (**2010**), Z. Naturforsch., Vol.65a, pp.1087 – 1092.
[25] Nandeppanavar, M.M., Vajravelu, K., Abel, M.S., and Siddalingappa, M.N., (**2012**), *Int. J. Thermal Sci.*, Vol. 58, pp. 143-150.
[26] Sajid, M., Ali, N., Abbas, Z., and Javed, T., (**2010**), *Int. J. Mod. Phys. B*, Vol.24, pp.5939-5947.
[27] Sahoo, B., and Poncet, S., (**2011**), *Int. J. Heat Mass Transfer*, Vol.54, pp.5010- 5019.
[28] Noghrehabadi, A., Pourrajab, R., and Ghalambaz, M., (**2012**), *Int. J. Thermal Sci.*, Vol.54, pp.253-261.
[29] Zheng, L., Niu, J., Zhang, X., and Gao, Y., (**2012**), *Math. Comp. Model.*, Vol.56, pp.133-144.
[30] Sharma, R., Ishak, A., Nazar, R., and Pop, I., (**2014**), *Journal of Applied Fluid Mechanics*, Vol. 7, No. 1, pp. 125-134.
[31] Rajesh Sharma and Anuar Ishak, (**2014**), *Wseas Transactions on Fluid Mechanics*, Vol. 9, pp.26-33.
[32] Andersson, H.I., Aarseth, J.B., Dandapat, B.S., (**2000**), *Int. J. Heat Mass Transfer*, Vol.43, pp.69-74.
[33] Shampine, L. F. and Kierzenka, J. (**2000**), Tutorial Notes.
[34] Ishak, A., Nazar, R., Pop, I., (**2009**), Meccanica, Vol.44, pp.369–375.